JOURNAL OF GEOPHYSICAL RESEARCH, VOL. 114, D08115, doi:10.1029/2008JD011157, 2009

Flux-gradient relationship of water vapor in the surface layer obtained from CASES-99 experiment

Sang-Jong Park,[1] Soon-Ung Park,[2] Chang-Hoi Ho,[1] and Larry Mahrt[3]

Received 17 September 2008; revised 16 December 2008; accepted 5 February 2009; published 25 April 2009.

[1] The flux-gradient relationship of water vapor Φ_q was obtained from the Cooperative Atmosphere-Surface Exchange Study-1999 (CASES-99) field experiment, which was conducted on a flat and grassy field in the southeastern part of Kansas, USA, during October 1999. The CASES-99 data include turbulence measurements of wind, temperature, and vapor density along with their time-averaged values at various levels above the ground. Quality control of the data on the turbulent wind velocity, sonic temperature, and vapor density was performed prior to flux calculation. The turbulent sensible heat and latent heat fluxes were calculated using a 30-min window, and they were subsequently corrected and checked for the fulfillment of the steady state and for turbulence intensity. Weak fluxes and through-tower wind data were also excluded from the analysis. Vertical gradients of the mean values were obtained by differentiating functions fitted to the measured mean profiles. It was found that Φ_q is comparable to Φ_T for weakly stable stratification and less than Φ_T for strongly stable stratification. On the contrary, Φ_q was found to be larger than Φ_T by approximately 20% for the neutral and unstable stratifications. The best fitting functions for water vapor are found to be $\Phi_q = 1.21(1 - 13.1z/L)^{-1/2}$ and $\Phi_q = 1.21(1 + 60.4z/L)^{1/3}$ for the unstable and stable stratifications, respectively.

Citation: Park, S.-J., S.-U. Park, C.-H. Ho, and L. Mahrt (2009), Flux-gradient relationship of water vapor in the surface layer obtained from CASES-99 experiment, *J. Geophys. Res.*, *114*, D08115, doi:10.1029/2008JD011157.

1. Introduction

[2] Water vapor flux plays an important role in land-atmosphere interactions by transporting latent heat and water vapor, and thereby influencing the atmospheric circulation [*Entekhabi et al.*, 1996]. For understanding water vapor flux in the surface layer, it is necessary to obtain the flux-gradient relationship of water vapor Φ_q. This relationship links the vertical gradient and flux of water vapor to atmospheric stability and has been used to obtain the vertical flux from a mean profile [*Beljaars*, 1982; *Asanuma et al.*, 2000; *Gieske*, 2003] and vice versa [*Gryning et al.*, 2007]. Numerical models for weather and climate also employ concepts of surface layer physics that involve the flux-gradient relationship [*Garratt*, 1993; *Pielke*, 2001].

[3] It is noted that water vapor fluxes obtained through numerical models and indirect measurements (e.g., the profile method, flux-variance method, and the Bowen ratio method) show larger errors than sensible heat fluxes determined through models and measurements [*Paulson et al.*, 1972; *Chen et al.*, 1996; *Betts et al.*, 1998; *Katul and Hsieh*, 1999; *Yang et al.*, 2006; *Steeneveld et al.*, 2008]. Considering that the flux-gradient relationship of water vapor has been used in flux parameterization, an accurate determination of the relationship may be one among many ways to reduce errors in calculations of the water vapor flux.

[4] However, the flux-gradient relationship of water vapor has not been sufficiently validated, while the flux-gradient relationships of wind and temperature have been validated in many experimental studies and reviews [*Dyer*, 1974; *Kader and Yaglom*, 1990; *Hogstrom*, 1996] even for extreme stabilities of free convective condition [*Grachev et al.*, 2000; *Wilson*, 2001] and very stable condition [*Beljaars and Holtslag*, 1991; *Zilitinkevich and Calanca*, 2000; *Chenge and Brutsaert*, 2005; *Grachev et al.*, 2007]. A few experimental studies have been conducted on Φ_q and these studies have suggested that its similarity with Φ_T [*Dyer*, 1967; *Francey and Garratt*, 1981; *Dyer and Bradley*, 1982; *Oncley et al.*, 1996; *Edson et al.*, 2004] exists for the unstable condition. Therefore the equality of the relationships may not be applicable to the neutral and stable conditions. Although *Pruitt et al.* [1973] examined Φ_q under the neutral, stable, and unstable conditions, they did not have Φ_T to compare their results and validate similarity between the two relationships.

[5] In order to validate the similarity between the scalar transfers, the ratio of the eddy diffusivity of water vapor to that of temperature has been studied instead of the flux-gradient relationship. Some studies have suggested that the eddy diffusivities of water vapor and temperature in the

[1]School of Earth and Environmental Sciences, Seoul National University, Seoul, Korea.
[2]Center for Atmospheric and Environmental Modeling, Seoul, Korea.
[3]College of Oceanic and Atmospheric Sciences, Oregon State University, Corvallis, Oregon, USA.

0148-0227/09/2008JD011157$09.00

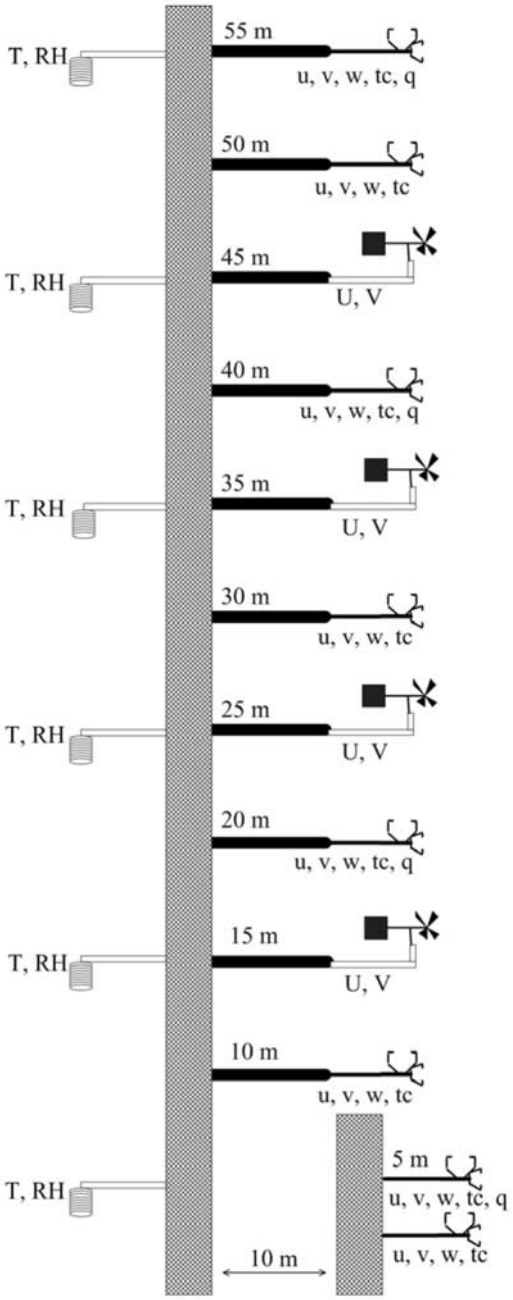

Figure 1. Schematic diagram of the main tower in the CASES-99 experiment. The capital lettered sensors are for obtaining mean values (*T*, temperature; RH, relative humidity; *U* and *V*, *x* and *y* component of horizontal mean wind). The small-lettered sensors are for measuring turbulence (*u*, *v*, *w*: three components of the wind speed; tc: sonic temperature; *q*: humidity).

atmosphere are similar [*Swinbank and Dyer*, 1967], but a possible dissimilarity is caused by the advection effect [*Blad and Rosenberg*, 1974; *Verma et al.*, 1978; *Lang et al.*, 1983]. Some studies reported the dissimilarity even in a non-advection environment [*Jacovides et al.*, 1988; *Papaioannou et al.*, 1989]. The difference in the buoyancy effects of temperature and water vapor might be the cause of the dissimilarity between the two physical quantities [*Warhaft*, 1976].

[6] The similarity between Φ_q and Φ_T is still a controversial subject, primarily because rare formula has been proposed on the basis of observations for Φ_q, a prerequisite to understand land-atmosphere interaction processes. The purpose of this study is to examine the flux-gradient relationship of water vapor using the experimental data obtained on a flat, homogeneous, grassy field. The details of the experiment and data processing are given in section 2. The obtained Φ_q is presented and compared with Φ_T in section 3. Finally, discussions involving previous studies are presented in section 4.

2. Data and Methodology

[7] In this section, we begin by providing details of the experimental environment and equipment. Then, methods of flux calculation, such as coordinate rotation and averaging time are described along with corrections applied to the calculated fluxes. Subsequently, quality control on turbulent heat fluxes using a basic test, a statistical test, and surface energy balance closure is explained, and this is followed by a description of the calculation of the vertical gradient from the fitted functions. Finally, the process of selecting high-quality data on the basis of various criteria is explained.

2.1. CASES-99 Experiment

[8] The Cooperative Atmosphere Surface Exchange Study-1999 (CASES-99) field experiment was conducted during October 1999 in southeastern Kansas. The experimental site had a flat terrain homogeneously covered with short grass. The site had a roughness length for momentum z_{0m} of 0.037 (±0.019) m. A 60-m tall main tower was located at 37.6486°N, 96.7351°W at an elevation of 432 m above sea level. Sensors for the profiles of the mean wind were installed at four heights from the ground: 15, 25, 35, and 45 m; temperature and relative humidity sensors were installed at six heights from the ground: 5, 15, 25, 35, 45, and 55 m. Three-dimensional sonic anemometers were also installed at the following eight heights in order to measure the momentum and sensible heat fluxes: 1.5, 5, 10, 20, 30, 40, 50, and 55 m. In particular, water vapor fluxes were measured at four heights: 5, 20, 40, and 55 m (Figure 1). Around the main tower, six 10-m towers (hereafter referred to as subtowers) were located at distances of 100 m and 300 m in three directions. The subtowers were equipped with flux sensors placed at a height of 5 m from the ground and with temperature and humidity sensors at a height of 2 m from the ground. The radiation and ground heat flux were also measured at the subtowers.

[9] The weather condition during the experimental period was fair, with mean winds blowing mostly from the south or the southwest. The footprint analysis [*Hsieh et al.*, 2000] showed that the main source areas for the fluxes measured at the 5-m height were most frequently around 50 m and 250 m distant upwind in unstable and stable conditions, respectively. The main source areas for the fluxes measured at the 20-, 40-, and 55-m heights were most frequently located around 150 m, 200 m, and 300 m, respectively, in the unstable condition and were located around 1500 m, 3500 m, and 6000 m, respectively, in the stable condition.

[10] The CASES-99 data on turbulence fluxes at multiple heights and on water vapor, temperature, and wind profiles have been used to study the flux-gradient relationships of temperature and momentum [*Chenge and Brutsaert*, 2005; *Steeneveld et al.*, 2005; *Ha et al.*, 2007] and to validate model results [*Steeneveld et al.*, 2008]. A more comprehensive description of the CASES-99 campaign can be found in the work of *Poulos et al.* [2002].

2.2. Turbulent Fluxes

[11] Turbulence measurements at high frequencies usually contain some abnormal data points. Therefore it is recommended to check the turbulence time series data for possible abnormality. Further, in order to select only data corresponding to well-developed and steady state turbulence, statistical tests of the turbulence intensity and steadiness were performed. A variation of the calculated flux with the averaging time was quantified to see if 30-min is appropriate to represent the eddy flux.

2.2.1. Basic Test for Turbulence Data

[12] In this study, the following four tests among those described in the work of *Vickers and Mahrt* [1997] were employed: the absolute limit test, spike test, abrupt change test, and higher-moment test. The absolute limit test detects unrealistic values in the time series. Each data point is compared to predefined minimum and maximum values: a maximum of 30 m s^{-1} for the horizontal wind speed and 5 m s^{-1} for the vertical wind speed, −20 and 50°C for the air temperature, and 0 and 50 g m^{-3} for the vapor density. A block of 30-min turbulence time series data is soft flagged when the number of data points outside the predefined range is less than the 2.5% of the total number of points, and the data are hard flagged if the number of data points outside the predefined range is more than 2.5% of the total number of points.

[13] In the spike test, a point is labeled a "spike" if it lies beyond the threshold of 3.25 times standard deviation from the mean of the 30-min record, and the point is linearly interpolated with surrounding points. When data points for an interval greater than 5 s continue to lie outside the threshold, they are soft flagged for further inspection. The detection process is repeated until no spikes are detected; the threshold is increased by 10% for every successive process. If the number of spikes detected exceeds 2.5% of the total number of data points, the data are hard flagged and excluded from the analysis. The spike test was performed for a non-overlapping window.

[14] Abrupt changes in the time series data are detected using the Haar transform [*Howell and Mahrt*, 1994]. For every point, the difference between the mean values of the data over two half-windows is compared to the 3.25 times of mean standard deviations of both the half-windows. If the difference around any point is greater than the threshold, the abovementioned record is soft flagged, and if the number of points soft flagged is more than 2.5% of the total number of points in a 30-min record, then the record is hard flagged. This test was performed for an overlapping window of 30-min length that was moving by one point at a time.

[15] The moments of the data are used to detect possible problems. The probable ranges (the minimum and maximum values) of each moment are predefined. The data is hard flagged if the skewness of the data is out of the range (−3.6, 3.6) or the kurtosis is out of the range (0.4, 14.4). The record is also hard flagged when the standard deviations of the following variables are out of their corresponding ranges: (0.01, 4) for horizontal wind velocities (0.01, 3) for vertical wind velocity; (0.01, 0.5) for air temperature, and (0.01, 0.5) for vapor density. These limits are chosen such that they are not very stringent and do not affect the results of this study.

2.2.2. Flux Calculation and Correction

[16] Prior to flux calculation, the direction of the wind velocities was varied using the planar fit method [*Wilczak et al.*, 2001]. Eighty four sets of 30-min wind-velocity data were used to obtain the regression plane for each day, and the rotation was performed on a daily basis. The resulting rotation angles were no more than one degree, confirming that the terrain was flat. The data were not detrended in order to retain possible contributions of large eddies [*Finnigan et al.*, 2003; *Lee et al.*, 2004a]. The analysis of the data was carried out using block averages of 30 min. This averaging time was selected for two reasons. It is the most commonly used time interval in studies of the flux-gradient relationship, and hence this selection makes our analysis consistent to previous studies. An analysis of the variation of the fluxes with the averaging time also showed that this timescale contains the contributions of eddies of almost all sizes. An example of the monthly averaged daytime flux variation is shown in Figure 2. It is also noted that a longer averaging period is necessary to obtain adequate flux at higher altitudes and under unstable conditions.

[17] Several steps and specific equations for the correction of the water vapor flux and sensible heat flux are described in the study by *Oncley et al.* [2007] and brief descriptions are given below. To correct the sensible heat flux, sonic temperature was converted into the actual temperature by accounting for the effect of water vapor [*Schotanus et al.*, 1983].

[18] As the first step in the water vapor flux correction, the cross-sensitivity to oxygen molecules was corrected [*van Dijk et al.*, 2003] and required extinction coefficients were given in the field logbook of the CASES-99 which is available at http://www.eol.ucar.edu/rtf/projects/cases99/isff.html. After correction for oxygen absorption, the vapor density measured with the krypton hygrometer was corrected for the different air densities of the ascending and descending air parcels [*Webb et al.*, 1980]. As the last step, the attenuation of the water vapor flux due to sensor displacement is corrected using the cospectral function of *Horst* [1997], empirical relations for the peak frequencies [*Horst*, 2003], and the elliptical shape of the turbulent eddies [*Lee and Black*, 1994].

[19] Because of the interdependency between the sensible heat flux and the latent heat flux, the above correction process was iterated until the flux change was less than 0.05 W m^{-2}. In this analysis, convergence was usually accomplished within three iterations. After correction, the latent heat fluxes typically increased at most by 20 W m^{-2} (30%), while the sensible heat fluxes decreased at most by 5 W m^{-2} (5%) under the unstable condition. For the stable condition, the flux correction was less than 5 W m^{-2}.

2.2.3. Statistical Test for Turbulence Data

[20] Since the flux-gradient relationship is based on the Monin-Obukhov similarity (MOS), it is required that the

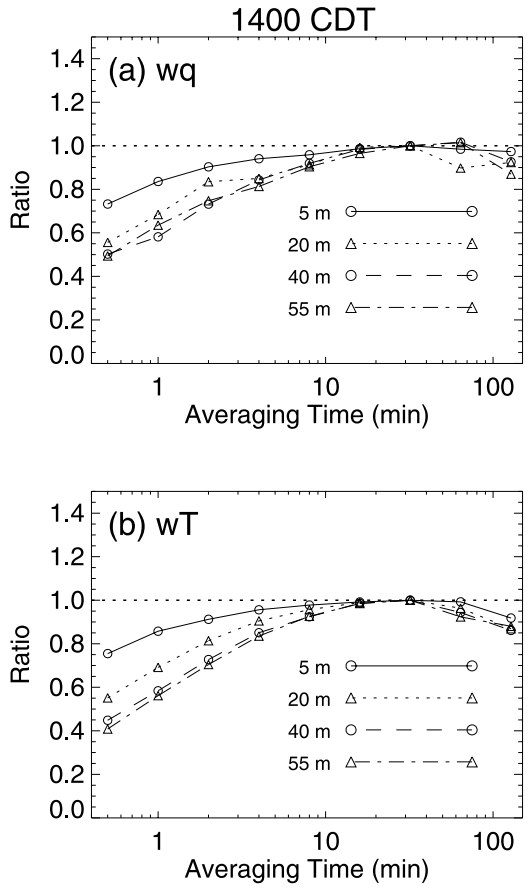

Figure 2. Monthly mean variations of (a) water vapor flux and (b) heat flux shown according to the averaging time. The fluxes are normalized by fluxes with an averaging time of 32 min. The shortest time is 0.5 min (30 s), and the time is doubled for each symbol to a maximum of 128 min (~2 h).

turbulence be well developed and in the steady state. The non-fulfillment of this ideal condition is regarded as one of the causes for an increase in the uncertainty in the parameterization of turbulent transport. Therefore it is recommended that for fundamental research purposes, high-quality turbulence data checked for two statistical quantities (the steady state ratio [SST] and integral turbulence characteristic [ITC]) be used [*Foken and Wichura*, 1996; *Mauder and Foken*, 2004].

[21] For the steady state test (SST), the 30-min-long data was divided into six subsections of 5-min data. Then, the difference between the average of the covariance of the six subsections and the covariance of the entire 30-min record is normalized by the latter. Time series data are considered to be steady state data if this ratio is lower than 30%.

[22] The integral turbulence characteristic (ITC) is used along with the steady state test to qualify turbulence data. The degree of turbulence development is determined using the flux-variance, the non-dimensional ratio of the standard deviation to the scaling parameter of a turbulent quantity. The "model" ITC was calculated using the flux-variance functions [*Lee et al.*, 2004a]. The difference between the "model" ITC and the observed ITC was normalized by the former. The data is regarded to have well-developed turbulence if the difference is lower than 30%.

[23] The monthly averaged diurnal variations of the ITC for vertical velocity and SST for vertical velocity, temperature, and water vapor measured at the 5-m height are shown in Figure 3. It is noted that the momentum flux data are of high quality in both the ITC and SST test; there are some unsteady data for nighttime. According to the SST test, most of the heat flux data for daytime are considered to be of high quality, but during nighttime, a considerable part of the heat flux and vapor flux data are not in steady state.

2.2.4. Surface Energy Balance

[24] The energy balance closure can be used to examine the overall characteristics of the experiment such as the quality of flux measurements, local advection caused by the heterogeneity of the environment, and large-scale transport of heat or vapor [*Lee et al.*, 2004b; *Oncley et al.*, 2007]. To evaluate the surface energy balance, the heat flux at the surface G_{sfc} was calculated by adding the soil heat storage S_{soil} to the soil heat flux $G_{\Delta z}$ measured at a depth of Δz. The soil heat storage was calculated as

$$S_{soil} = -C_v \frac{\partial Tsoil}{\partial t} \Delta z, \tag{1}$$

where T_{soil} is the soil temperature. The volumetric heat capacity C_v was calculated as

$$C_v = \sum \rho_i Cp_i f_i = 1600 \times 1900 \times f_{\min} + 600 \times 2500 \times f_{org} + 1000 \times 4218 \times f_{wat} [\mathrm{J\ m^{-3}\ K^{-1}}], \tag{2}$$

where ρ_i, C_{pi}, and f_i are the density, specific heat capacity, and volumetric fraction of matter i, respectively; the fractions of mineral and organic matter are $f_{\min} = 0.55$ and $f_{org} = 0.01$ (*Oncley*, 2005, personal communication). Soil heat flux $G_{\Delta z}$ was measured at a depth of 5 cm, and T_{soil} was measured at a depth of 1–4 cm. Because there was no soil heat flux measurement at the main tower, the soil heat flux at subtower 1 was used for determining the surface energy balance since the surface conditions at both sites were similar [*Sun et al.*, 2003].

[25] The surface energy balance was examined by comparing the sum of the sensible heat flux, latent heat flux, and the ground surface heat flux to the net radiation at the surface (Figure 4). The surface energy balance was closed within 5%, indicating the good quality of turbulent fluxes as well as the homogeneity of the surrounding environment.

2.3. Vertical Gradient

[26] The flux-gradient relationship of water vapor is defined using the specific humidity, which is calculated from the relative humidity, air temperature, and air pressure. In this study, the saturation vapor pressure was calculated from the air temperature and atmospheric pressure [*Buck*, 1981]. The atmospheric pressures at each height were calculated using the pressure measured at the heights of 1.5 m and 30 m. The potential temperature was also calculated using the air temperature and air pressure.

[27] The lowest heights at which the temperature and humidity sensors were positioned in the main tower were the same as the lowest height at which flux measurements

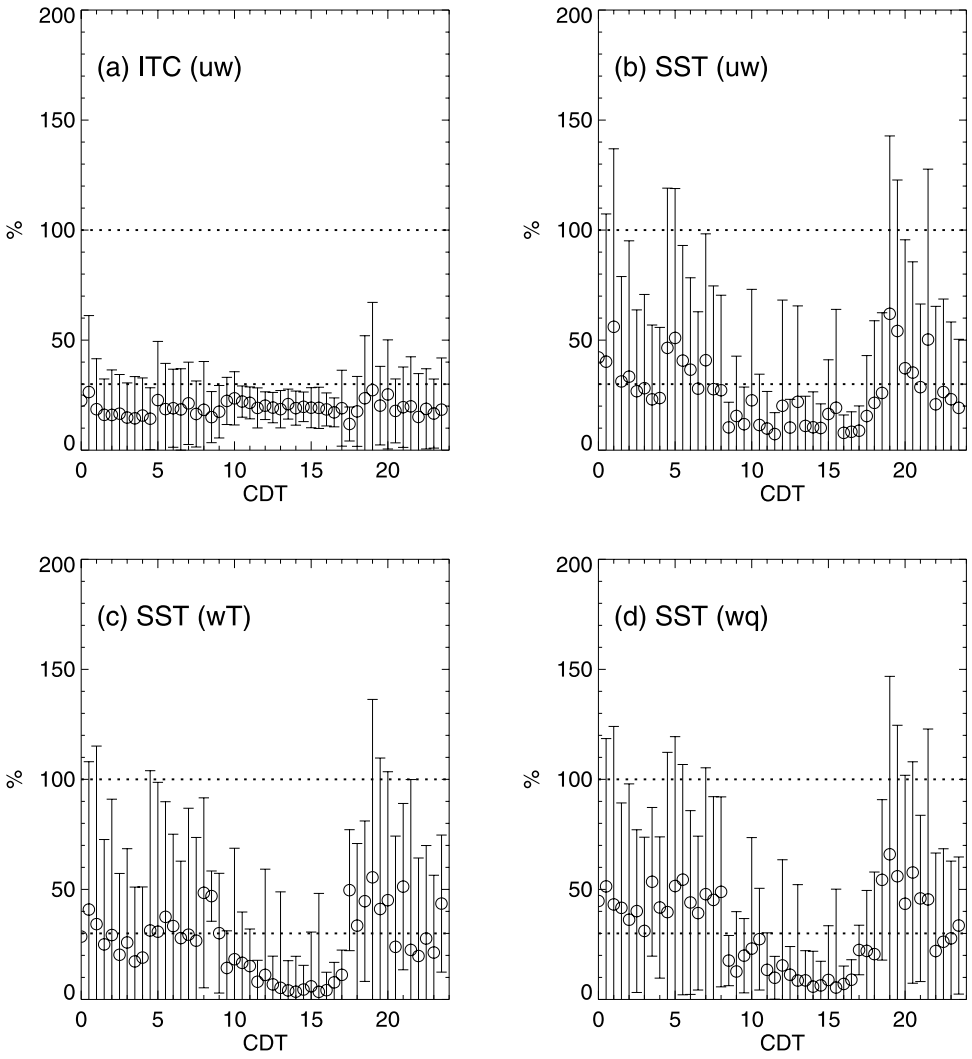

Figure 3. Monthly mean diurnal variations of (a) uw ITC, (b) uw SST, (c) wT SST, and (d) wq SST measured at the 5-m height. Dotted lines denoting 30% and 100% are drawn to show thresholds for statistical quality control.

were obtained (5 m). In this study, the temperature and humidity values measured at the 2-m height on the six subtowers were averaged and incorporated into the profiles of temperature and humidity in order to avoid the probable erratic gradient at the lowest height in the main tower.

[28] The vertical profiles of temperature and humidity were fitted to three kinds of functions: the log linear function (LLN [*Howell and Sun*, 1999]), log-square function (LSQ [*Oncley et al.*, 1996]), and log-cubic function (LCB [*Steeneveld et al.*, 2005]). These functions are given below:

$$X(z)_{LLN} = A + B\ln(z) + Cz, \tag{3a}$$

$$X(z)_{LSQ} = A + B\ln(z) + C\ln^2(z), \tag{3b}$$

$$X(z)_{LCB} = A + B\ln(z) + C\ln^2(z) + D\ln^3(z), \tag{3c}$$

where $X(z)$ is a variable to be fitted at the height of z. After determining the coefficients in the fitting functions, the vertical gradients were calculated by the differentiation of these functions.

[29] The sensitivities of the vertical gradients to the different fitting methods (equation (3)) were investigated. As shown in Figure 5, the gradients for both water vapor and temperature at the 5-m height were not sensitive to the fitting methods and the gradient obtained from the different fitting methods varied by not more than 3% on average. At levels higher than 5 m, however, large differences were observed among the results for different fitting functions, thereby increasing the uncertainty in the gradients at large heights.

2.4. Data Selection

[30] To ensure the high-quality data for the purpose of carrying out fundamental research, unsuitable data were excluded from the analysis on the basis of four criteria: quality control results, small flux threshold, goodness of fit to the profile, and wind direction. First, the hard flagged

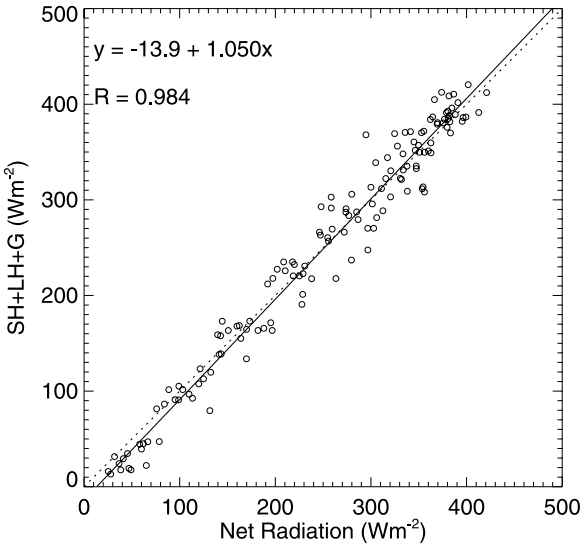

Figure 4. Comparison of net radiation to the sum of fluxes (sensible heat flux + latent heat flux + ground heat flux). The solid line represents the linear regression time and the dotted line denotes the 1:1 line.

data in the basic tests described in section 2.2.1 were excluded. Records were also excluded if the ITC deviation or SST deviation was greater than 30%, as described in section 2.2.3. Here in accordance with the 2004 Spoleto Agreement for CarboEurope-IP [*Mauder and Foken*, 2004], the ITC test was applied only for the momentum flux, but the SST was applied for the momentum, sensible heat, and water vapor fluxes. Second, small fluxes were excluded using the following threshold values: 0.025 m s^{-1}, 5 W m^{-2}, and 2 W m^{-2} for the friction velocity, sensible heat flux, and latent heat flux, respectively. The threshold value for the latent heat flux was determined to include as many data points as possible while not distorting the overall characteristic of the flux-gradient relationship of water vapor. Third, badly fitted profiles with large fitting errors were excluded from the analysis; the fitting error is defined as the ratio of the root mean square error (RMSE) of the fit to the range of values in the profile. Such a relative fitting error provides a better criterion for the goodness of fit of a profile as compared to the RMSE; the relative fitting error is equally applicable to the daytime and nighttime profiles, while the RMSE tends to be small for the well-mixed daytime profile. Fourth, disturbed turbulences in the through-tower wind direction (270° ± 30°) were excluded.

[31] In addition to the above criteria, measurements obtained after 28 October were not included because of the rainy weather. Moreover, measurements obtained at the 20-, 40-, and 55-m heights were not included in the result because of the following three reasons: (1) the possible effect of the pond located approximately 120 to 200 m away, which might have partially overlapped with the main source areas of fluxes; (2) the large uncertainty in the vertical gradient depending on the fitting functions as stated in section 2.3, and (3) the low surface layer height in the stable nighttime conditions. The flux-gradient relationship should be analyzed for the surface layer data in order to meet the MOS assumption.

[32] Only the fluxes measured at the 5-m height until 28 October were used in further analysis. Consequently, from the 1344 data points (48 data points × 28 days) that were available for the 5-m height, approximately 33% (447 data points) and 42% (558 data points) of the data were included in the analysis of the flux-gradient relationships of water vapor and temperature, respectively (Table 1).

3. Results

[33] Turbulent fluxes and the vertical gradients of water vapor were combined to determine the flux-gradient relationship of water vapor as:

$$\Phi_q = \frac{kz}{q_*}\frac{\partial Q}{\partial z} \tag{4}$$

where Q is the mean specific humidity, q_* is the scaling parameter for water vapor flux, k is the von Karman constant, and z is the height above the surface. The flux-gradient relationship of temperature was also estimated in the same way to validate the similarity between water vapor and temperature. Because of different vertical gradients yielded by the three fitting methods (equation (3)), flux-gradient relationships were analyzed separately for each fitting method. After formulating the flux-gradient relationships as functions of stability, these new functions were compared with the selected reference functions from those in the literature.

3.1. Flux-Gradient Relationships of Water Vapor and Temperature

[34] The estimated flux-gradient relationships of water vapor and temperature from the 5-m-height data using the LCB fitting method are shown in Figure 6 according to the atmospheric stability. It is noted that removing the outlying data in the original distribution (Figures 6a and 6c) after data selection (Figures 6b and 6d) made the flux-gradient relationships much more coherent. Reference functions for temperature are shown alongside.

[35] On the basis of the estimated values shown in Figure 6, a Businger-Dyer type function was used to formulate the flux-gradient relationship of water vapor for the unstable as well as the stable condition. A Businger-Dyer type function is given by

$$\Phi_q = A_q\left(1 + B_q\frac{z}{L}\right)^{\wedge} C_q, \tag{5}$$

where q represents water vapor; A_q, B_q, and C_q are empirical coefficients to be determined; and z/L is the atmospheric stability.

[36] The empirical coefficients were determined by the following process, starting with A_q and C_q since they can be obtained independently. First, A_q was determined using the observed Φ_q values for the near-neutral condition ($-0.05 \leq z/L \leq 0.05$) because Φ_q in equation (5) is equal to A_q for neutral stability ($z/L \rightarrow 0$). C_q was determined from the slope of the linear regression line between the logarithms of Φ_q and $|z/L|$. This linear regression is acceptable for a sufficiently large $|z/L|$ since the magnitude of B_q is presumably around ten. After A_q and C_q were determined, B_q was

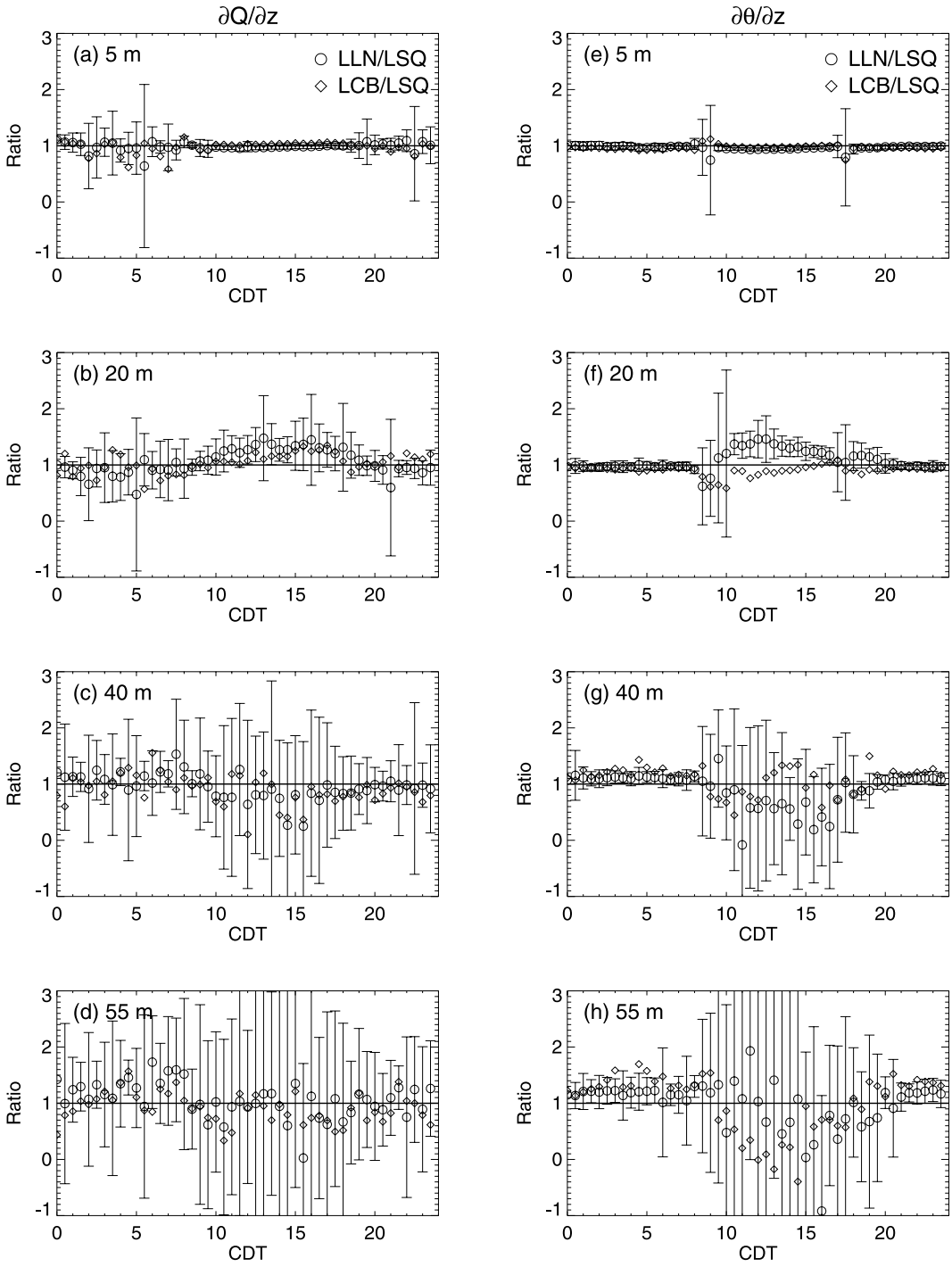

Figure 5. Diurnal variation of the monthly mean ratio of the vertical gradients of specific humidity (Q) and potential temperature (θ). Vertical gradients obtained using the log linear (LLN, open circle) and log-cubic (LCB, diamond) methods are normalized by those obtained using the log-square (LSQ) method. The error bar represents the standard deviation of the ratio of the values obtained from the LLN method to those obtained from the LSQ method.

determined through regression by considering all the Φ_q values and by minimizing the root mean square error. The values of A_q and C_q determined from the 5-m-height data by using the LCB fitting method are shown in Figure 7.

[37] The coefficients obtained through the above fitting process are given in Table 2. Note that the coefficients for the three profile-fitting methods agree well with each other. The coefficient C_q was set to $-1/2$ and $+1/3$, which were close to the fitted values for the unstable and stable conditions, respectively, and B_q was determined accordingly without increasing the fitting error.

Table 1. Number of Excluded and Selected Data for the Flux Measurement and Vertical Gradient Obtained at a Height of 5 m and With Log-Cubic Fitting Method

	Criteria	Water Vapor	Temperature
Excluded data	Basic test	712	339
	Statistical test	518	468
	Small flux	250	215
	Bad fitting (LCB method)	46	48
	Through tower	95	95
Selected data		447	558

[38] The coefficients for the three profile-fitting methods were averaged to yield a single value, and the optimally fitted functions for Φ_q and Φ_T are given as

$$\Phi_q = 1.21\left(1 - 13.1\frac{z}{L}\right)^{-1/2} \text{ for unstable condition } (z/L < 0), \quad (6a)$$

$$\Phi_q = 1.21\left(1 + 60.4\frac{z}{L}\right)^{1/3} \text{ for stable condition } (z/L > 0), \quad (6b)$$

$$\Phi_T = 1.00\left(1 - 13.3\frac{z}{L}\right)^{-1/2} \text{ for unstable condition } (z/L < 0), \quad (7a)$$

$$\Phi_T = 1.00\left(1 + 27.5\frac{z}{L}\right)^{1/2} \text{ for stable condition } (z/L > 0). \quad (7b)$$

3.2. Comparison With the Flux-Gradient Relationship of Temperature

[39] Obtained Φ_q and Φ_T were compared to examine the assumption that the flux-gradient relationships of scalars are similar. Further, Φ_q was compared to the reference functions of *Hogstrom* [1996] and *Beljaars and Holtslag* [1991] for the unstable and stable conditions, respectively; the comparison was made with the following widely used functions:

a) Hogstrom function

$$\Phi_T = Pr_{t0}\left(1 - 11.6\frac{z}{L}\right)^{-1/2} \text{ for } z/L < 0, \quad (8)$$

b) Beljaars and Holtslag function

$$\Phi_T = Pr_{t0}\left[1 + \frac{z}{L}\left\{a\left(1 + \frac{2}{3}a\frac{z}{L}\right)^{1/2} + b\exp\left(-d\frac{z}{L}\right)\left(1 + c - d\frac{z}{L}\right)\right\}\right] \text{ for } z/L > 0, \quad (9)$$

where the coefficients are $a = 1$, $b = 0.667$, $c = 5$, and $d = 0.35$; Pr_{t0} is the turbulent Prandtl number for the neutral condition and has a value of 0.95 [*Hogstrom*, 1996].

[40] The newly obtained Φ_q and Φ_T along with the reference functions (equations (8) and (9)) are shown in

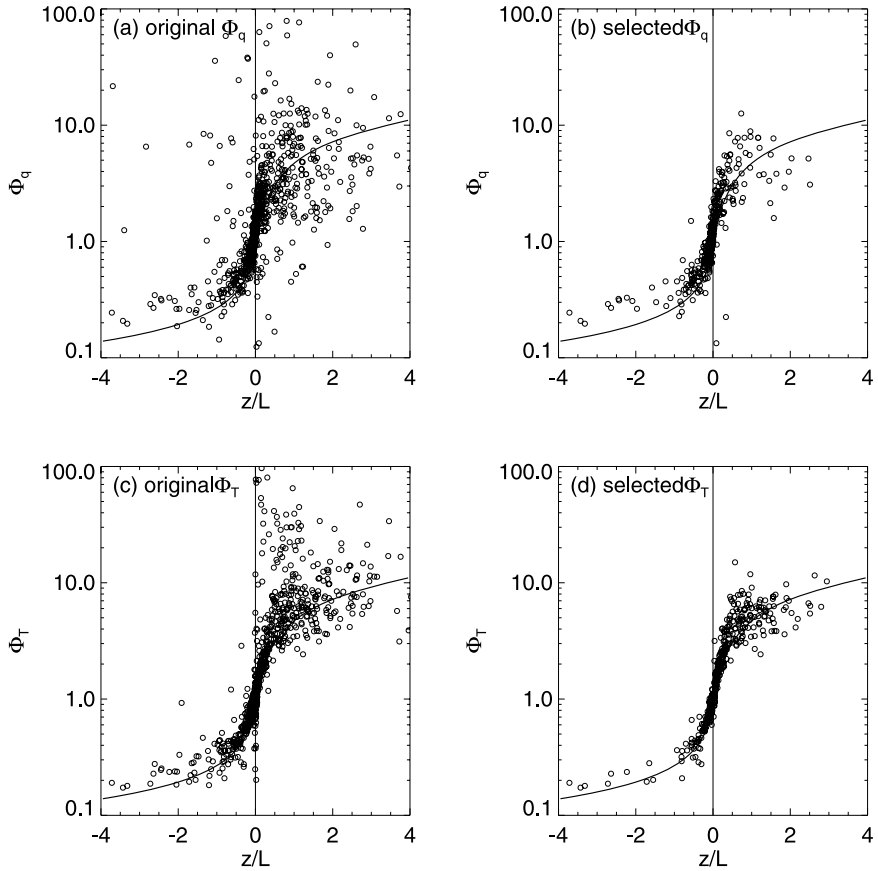

Figure 6. (top) The flux-gradient relationships of water vapor and (bottom) temperature at the 5-m height obtained using the log-cubic fitting method. (left) Original data. (right) Selected data. The flux-gradient relationships by *Hogstrom* [1996] and *Beljaars and Holtslag* [1991] are used as references for the unstable and stable conditions, respectively.

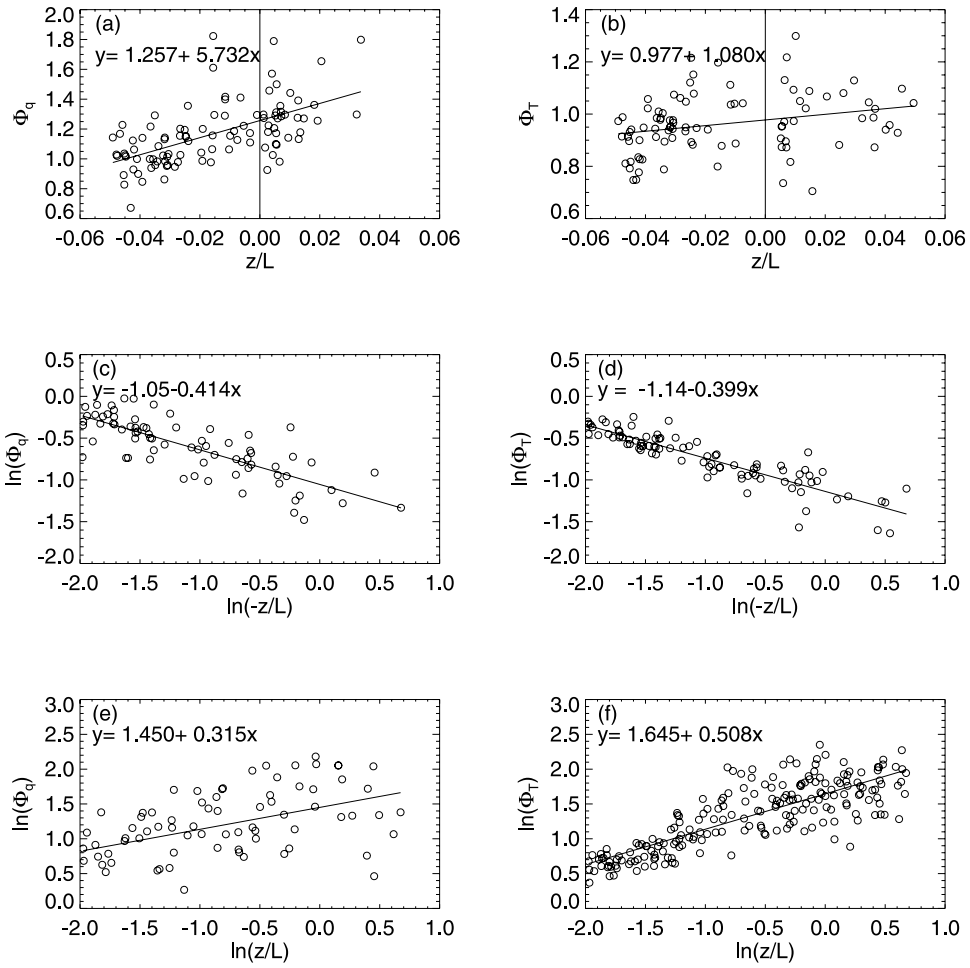

Figure 7. Determination of the coefficients A and C for (left) water vapor and (right) temperature from the 5-m-height data using the log-cubic fitting method. The coefficients (a) A_q and (b) A_T were obtained at $z/L = 0$ with C_q and C_T obtained from the slopes in Figures 7c and 7d for unstable stratification and Figures 7e and 7f for the stable stratification.

Figure 8. It is noted that Φ_T agrees very well with the reference functions over the entire stability range except for the weakly stable condition. Thus, considering the range of variation in the literature, Φ_T obtained in the present study does not represent a new function. The turbulent Prandtl number for the neutral limit is 1.00 (±0.01), which is within the range of values reported in the literature [*Hogstrom*, 1996; *Foken*, 2006].

[41] On the other hand, a discrepancy of approximately 20% is observed between Φ_q and the reference function for the unstable and neutral conditions. For the stable condition, however, the abovementioned discrepancy decreases at strongly stable condition of $z/L > 1$. The turbulent Schmidt number, defined as the ratio of the eddy diffusivity of water vapor to that of the momentum, is 1.21 (±0.02) for the neutral condition, indicating a dissimilarity between water vapor and temperature considering the turbulent Prandtl number of 1.00 (±0.01). This is an addition of data for determination of Schmidt number [*Foken*, 2006].

[42] The ratio of Φ_q to Φ_T is shown in Figure 9. The ratio is certainly larger than unity for the unstable condition, and then it decreases for the neutral condition to be around unity

Table 2. Coefficients Obtained After Fitting Flux-Gradient Relationships of Water Vapor and Temperature

		Water Vapor (Φ_q)			Temperature (Φ_T)		
Stability	Fitting	A_q	C_q	B_q	A_T	C_T	B_T
Unstable	LLN	1.16 (±0.02)	−0.45 (±0.05)	−13.5 (±0.7)	1.00 (±0.01)	−0.45 (±0.03)	−13.4 (±0.4)
	LSQ	1.22 (±0.02)	−0.43 (±0.04)	−10.5 (±0.7)	1.01 (±0.01)	−0.42 (±0.03)	−13.0 (±0.3)
	LCB	1.26 (±0.02)	−0.41 (±0.03)	−15.2 (±0.6)	0.98 (±0.01)	−0.40 (±0.03)	−13.6 (±0.3)
Stable	LLN		0.32 (±0.08)	61.4 (±6.9)		0.48 (±0.02)	25.9 (±1.0)
	LSQ		0.34 (±0.08)	61.5 (±7.1)		0.54 (±0.02)	30.2 (±1.2)
	LCB		0.32 (±0.08)	58.2 (±6.6)		0.51 (±0.02)	26.5 (±1.0)

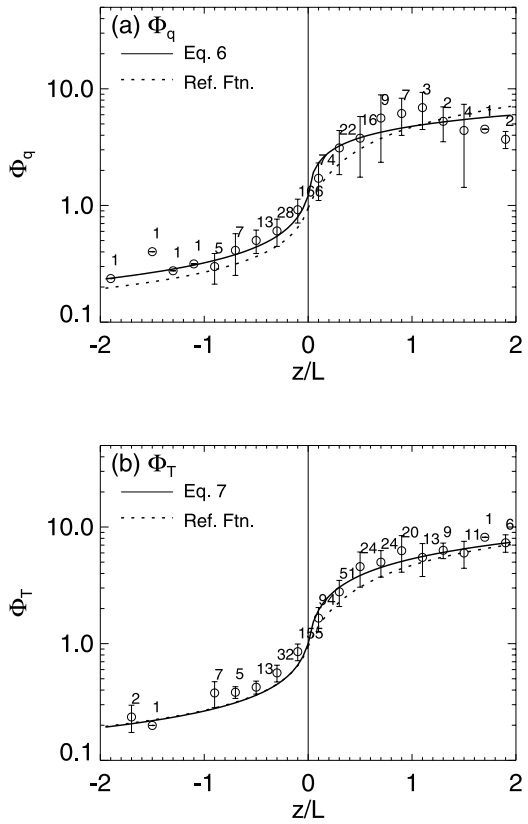

Figure 8. The flux-gradient relationships of (a) water vapor and (b) temperature at the 5-m height obtained using the log-cubic fitting method. The number of data in each stability bin is shown above the symbol. The solid lines are for the optimally fitted functions (equations (6) and (7)), and the dotted lines represent reference functions (equations (8) and (9)).

for the moderately stable condition. Inequality of eddy diffusivities of water vapor (K_q) and temperature (K_T) is shown in Figure 10. The observed K_T is overall larger than K_q for the unstable condition, while K_q becomes similar to and a little larger than K_T for the stable condition. The same information is given in the log-scale in Figure 10b. This clearly indicates that K_T is smaller than K_q under stable stability. Above variation of eddy diffusivities confirms the result of *Warhaft* [1976], who argued that the ratio of the eddy diffusivities of water vapor and temperature may depart from unity because of the different buoyancy effects of temperature and vapor fluctuation.

4. Summary and Discussion

[43] The flux-gradient relationships of water vapor and temperature were analyzed from the CASES-99 experiment that was conducted on a flat, homogeneous surface covered with short grass. Analysis using high-quality data showed that Φ_q was comparable to Φ_T for the weakly stable condition and less than Φ_T for the strongly stable condition. On the contrary, Φ_q was larger than Φ_T by about 20% for the neutral and unstable conditions. The observed Φ_q was formulated as a function of atmospheric stability and was compared to Φ_T to reveal dissimilarity between scalar transfers in terms of flux-gradient relationship.

[44] The results presented in this paper disagree with the equality of the flux-gradient relationships of water vapor and temperature [*Dyer*, 1967; *Francey and Garratt*, 1981; *Dyer and Bradley*, 1982]; different functions are suggested for each flux-gradient relationship.

[45] On the other hand, the abovementioned results agree with the experimental study of *Edson et al.* [2004] in that Φ_q at the neutral condition was 1.11 (±0.22) with a maximum of 1.36; this value is close to the value of 1.21 (±0.02) obtained in this study. Further, the result of *Warhaft* [1976] implied that Φ_q can be larger and smaller than Φ_T for the unstable and stable conditions, respectively. However, small number of data points and large deviation in the stable condition makes it difficult to decisively determine whether Φ_q is smaller than Φ_T, as reported by *Warhaft* [1976], or whether the two relationships are equal, as shown by *Dias and Brutsaert* [1996].

[46] Because of the following reasons, the dissimilarity between Φ_q and Φ_T reported in this study does not appear to have been caused by an advection effect, as suggested in other studies [*Bink*, 1996; *Lee et al.*, 2004b]. The CASES-99 site was flat and nearly homogeneously covered with short grasses with no drastic surface changes around the main tower. The surface energy balance was well closed, which is very rare in an advection environment. Φ_T obtained in this study exactly matched the reference functions for the unstable condition. Φ_q did not show a dependency on the wind direction. Abovementioned points indicate that the results in this paper should be regarded to correspond to an ideal environment and not a disturbed environment.

[47] To test the artificial correlation caused by the shared variable in Φ_q and z/L, all the variables in Φ_q and z/L were randomly combined to make new Φ_q and z/L, which were compared to the real data [*Klipp and Mahrt*, 2004; *Baas et al.*, 2006]. The result indicates that there is no significant artificial correlation between Φ_q and z/L (not shown). Therefore Φ_q as a function of stability in the present study is not originated from the shared variable and has physical meaning and artificial correlation is not an issue in Φ_q formulation.

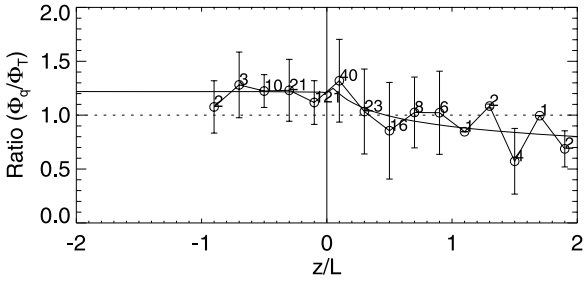

Figure 9. Bin averages of the ratio of the flux-gradient relationship of water vapor to that for temperature at the 5-m height obtained using the log-cubic fitting method. The number of data in each stability bin of $\Delta z/L = 0.2$ is shown above the symbol. The solid line represents the ratio of the fitted functions (equations (6) and (7)).

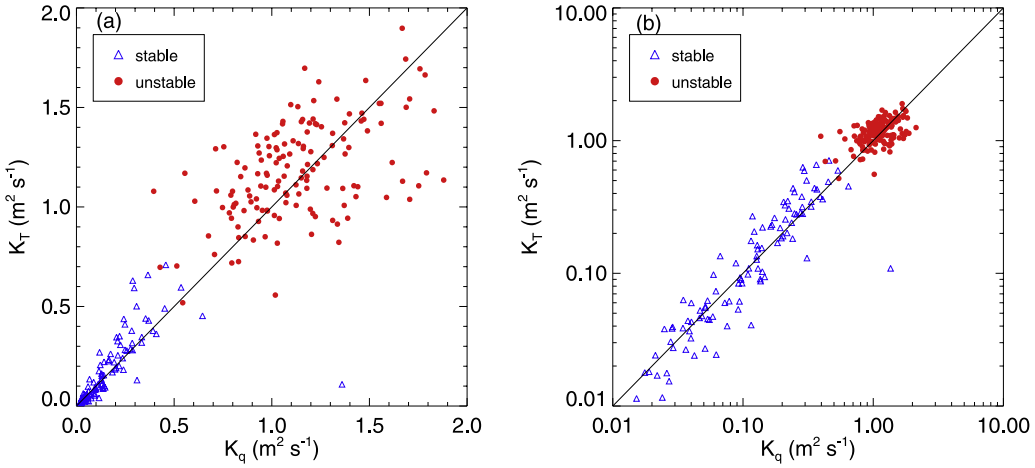

Figure 10. Eddy diffusivities of water vapor (K_q) and temperature (K_T) estimated from observations for the unstable condition (solid circle) and stable condition (triangle) are shown in (a) a linear scale and (b) the log scale.

[48] Our results indicate that the efficiency of the turbulent transport of water vapor is lower than that of temperature for the unstable condition, but is comparable or higher for the stable condition. The reason for the different transport efficiency of water vapor and temperature is thought to be the different buoyancy effect of water vapor and temperature (i.e., active/passive scalar) as suggested earlier [*Warhaft*, 1976; *Katul and Parlange*, 1994; *Asanuma and Brutsaert*, 1999; *Katul and Hsieh*, 1999; *Moriwaki and Kanda*, 2006].

[49] Considering the dissimilarity between water vapor and temperature, we should be aware of possible errors caused by dissimilarities between scalars in flux measurements (e.g., those of CO_2 and methane) that are based on similarities between scalars [*Meyers et al.*, 1996; *Rannik et al.*, 2004]. For example, Bowen ratio-energy balance method could overestimate the evaporation by about 7% to 13% for Bowen ratios being from 0.5 to 2.0 at moderately unstable condition. It should be studied further that which of water vapor and temperature shows closer similarity to other gases [*Moriwaki and Kanda*, 2006].

[50] Although Φ_q for the stable conditions was formulated using the Businger-Dyer-type function as for the unstable condition, other types of functions might be appropriate to formulate the same relationship [*Beljaars and Holtslag*, 1991; *Duynkerke*, 1999; *Chenge and Brutsaert*, 2005]. While it is well known that the $-1/3$ power law represents free convection regime [*Garratt*, 1992], $-1/2$ power law seems appropriate for the moderately unstable condition as obtained from the optimal regression in this study. Analysis on the behavior of Φ_q for the free convective regime was not available due to lack of data in the free convective regime. Moreover, since the results presented in this paper were obtained from only one set of experimental data, additional observational studies should be conducted in various environments to obtain a generalized function for water vapor, as in the case of temperature and momentum.

[51] **Acknowledgments.** This work was funded by the Korea Meteorological Administration Research and Development Program under grant CATER 2006-4204. The authors would like to thank the National Center for Atmospheric Research (NCAR), Earth Observing laboratory (EOL), and Joint Office for Science Support (JOSS) for their kindness in providing the CASES-99 data. We also thank S. Oncley and G. Maclean for their kind help regarding soil data and raw data processing, respectively.

References

Asanuma, J., and W. Brutsaert (1999), The effect of chessboard variability of the surface fluxes on the aggregated turbulence fields in a convective atmospheric surface layer, *Boundary Layer Meteorol.*, *91*(1), 37–50.

Asanuma, J., N. L. Dias, W. P. Kustas, and W. Brutsaert (2000), Observations of neutral profiles of wind speed and specific humidity above a gently rolling landsurface, *J. Meteorol. Soc. Jpn.*, *78*(6), 719–730.

Baas, P., G. J. Steeneveld, B. J. H. van de Wiel, and A. A. M. Holtslag (2006), Exploring self-correlation in flux-gradient relationships for stably stratified conditions, *J. Atmos. Sci.*, *63*(11), 3045–3054.

Beljaars, A. C. M. (1982), The derivation of fluxes from profiles in perturbed areas, *Boundary Layer Meteorol.*, *24*(1), 35–55.

Beljaars, A. C. M., and A. A. M. Holtslag (1991), Flux parameterization over land surfaces for atmospheric models, *J. Appl. Meteorol.*, *30*(3), 327–341.

Betts, A. K., P. Viterbo, A. Beljaars, H. L. Pan, S. Y. Hong, M. Goulden, and S. Wofsy (1998), Evaluation of land-surface interaction in ECMWF and NCEP/NCAR reanalysis models over grassland (FIFE) and boreal forest (BOREAS), *J. Geophys. Res.*, *103*(D18), 23,079–23,085.

Bink, N. J. (1996), The ratio of eddy diffusivities for heat and water vapour under conditions of local advection, *Phys. Chem. Earth*, *21*(3), 119–122.

Blad, B. L., and N. J. Rosenberg (1974), Lysimetric calibration of the Bowen ratio-energy balance method for evapotranspiration estimation in the Central Great Plains, *J. Appl. Meteorol.*, *13*(2), 227–236.

Buck, A. L. (1981), New equations for computing vapor pressure and enhancement factor, *J. Appl. Meteorol.*, *20*, 1527–1532.

Chen, F., K. Mitchell, J. Schaake, Y. Xue, H. L. Pan, V. Koren, Q. Duan, Y. Ek, and M. Betts (1996), Modeling of land surface evaporation by four schemes and comparison with FIFE observations, *J. Geophys. Res.*, *101*(D3), 7251–7268.

Chenge, Y., and W. Brutsaert (2005), Flux-profile relationships for wind speed and temperature in the stable atmospheric boundary layer, *Boundary Layer Meteorol.*, *114*(3), 519–538.

Dias, N. L., and W. Brutsaert (1996), Similarity of scalars under stable conditions, *Boundary Layer Meteorol.*, *80*(4), 355–373.

Duynkerke, P. G. (1999), Turbulence, radiation and fog in Dutch stable boundary layers, *Boundary Layer Meteorol.*, *90*(3), 447–477.

Dyer, A. J. (1967), The turbulent transport of heat and water vapour in the unstable atmosphere, *Q. J. R. Meteorol. Soc.*, *93*, 501–508.

Dyer, A. J. (1974), A review of flux-profile relations, *Boundary Layer Meteorol.*, *1*, 363–372.

Dyer, A. J., and E. F. Bradley (1982), An alternative analysis of flux-gradient relationships at the 1976 ITCE, *Boundary Layer Meteorol.*, *22*(1), 3–19.

Edson, J. B., C. J. Zappa, J. A. Ware, W. R. McGillis, and J. E. Hare (2004), Scalar flux profile relationships over the open ocean, *J. Geophys. Res.*, *109*, C08S09, doi:10.1029/2003JC001960.

Entekhabi, D., I. Rodriguez-Iturbe, and F. Castelli (1996), Mutual interaction of soil moisture state and atmospheric processes, *J. Hydrol.*, *184*(1-2), 3–17.

Finnigan, J. J., R. Clement, Y. Malhi, R. Leuning, and H. A. Cleugh (2003), A re-evaluation of long-term flux measurement techniques. part I: Averaging and coordinate rotation, *Boundary Layer Meteorol.*, *107*, 1–48.

Foken, T. (2006), 50 Years of the Monin-Obukhov Similarity Theory, *Boundary Layer Meteorol.*, *119*(3), 431–447.

Foken, T., and B. Wichura (1996), Tools for quality assessment of surface-based flux measurement, *Agric. For. Meteorol.*, *78*, 83–105.

Francey, R. J., and J. R. Garratt (1981), Interpretation of flux-profile observations at ITCE (1976), *J. Appl. Meteorol.*, *20*(6), 603–618.

Garratt, J. R. (1992), *The Atmospheric Boundary Layer*, 316 pp., Cambridge Univ. Press, New York.

Garratt, J. R. (1993), Sensitivity of climate simulations to land-surface and atmospheric boundary-layer treatments—A review, *J. Clim.*, *6*(3), 419–448.

Gieske, A. (2003), The iterative flux-profile method for remote sensing applications, *Int. J. Remote Sens.*, *24*(16), 3291.

Grachev, A. A., C. W. Fairall, and E. F. Bradley (2000), Convective profile constants revisited, *Boundary Layer Meteorol*, *94*(3), 495–515.

Grachev, A. A., E. L. Andreas, C. W. Fairall, P. S. Guest, and P. O. G. Persson (2007), SHEBA flux-profile relationships in the stable atmospheric boundary layer, *Boundary Layer Meteorol.*, *124*(3), 315–333.

Gryning, S.-E., E. Batchvarova, B. Brummer, H. Jorgensen, and S. Larsen (2007), On the extension of the wind profile over homogeneous terrain beyond the surface boundary layer, *Boundary Layer Meteorol.*, *124*(2), 251–268.

Ha, K.-J., Y.-K. Hyun, H.-M. Oh, K.-E. Kim, and L. Mahrt (2007), Evaluation of boundary layer similarity theory for stable conditions in CASES-99, *Mon. Weather Rev.*, *135*(10), 3474–3483.

Hogstrom, U. (1996), Review of some basic characteristics of the atmospheric surface layer, *Boundary Layer Meteorol.*, *78*, 215–246.

Horst, T. W. (1997), A simple formula for attenuation of eddy fluxes measured with first-order response scalar sensors, *Boundary Layer Meteorol.*, *82*, 219–233.

Horst, T. W. (2003), Attenuation of scalar fluxes measured with displaced sensors, paper presented at EGS-AGU-EGU Joint Assembly, Nice, France, 6–11 April.

Howell, J. F., and L. Mahrt (1994), An adaptive multiresolution data filter: Applications to turbulence and climatic time series, *J. Atmos. Sci.*, *51*, 2165–2178.

Howell, J. F., and J. Sun (1999), Surface-layer fluxes in stable conditions, *Boundary Layer Meteorol.*, *90*(3), 495–520.

Hsieh, C.-I., G. G. Katul, and T.-W. Chi (2000), An approximate analytical model for footprint estimation of scalar fluxes in thermally stratified atmospheric flows, *Adv. Water Resour.*, *23*, 765–772.

Jacovides, C., G. Papaioannou, and P. Kerkides (1988), Micro and large-scale parameters evaluation of evaporation from a lake, *Agric. Water Manage.*, *13*(2-4), 263–272.

Kader, B. A., and A. M. Yaglom (1990), Mean fields and fluctuation moments in unstably stratified turbulent boundary layers, *J. Fluid Mech.*, *212*, 637–662.

Katul, G. G., and M. B. Parlange (1994), On the active role of temperature in surface-layer turbulence, *J. Atmos. Sci.*, *51*(15), 2181–2195.

Katul, G. G., and C.-I. Hsieh (1999), A note on the flux-variance similarity relationships for heat and water vapour in the unstable atmospheric surface layer, *Boundary Layer Meteorol.*, *90*(2), 327–338.

Klipp, C. L., and L. Mahrt (2004), Flux-gradient relationship, self-correlation and intermittency in the stable boundary layer, *Q. J. R. Meteorol. Soc.*, *130*(601), 2087–2103.

Lang, A. R. G., K. G. McNaughton, C. Fazu, E. F. Bradley, and E. Ohtaki (1983), Inequality of eddy transfer coefficients for vertical transport of sensible and latent heats during advective inversions, *Boundary Layer Meteorol.*, *25*, 25–41.

Lee, X., and T. A. Black (1994), Relating eddy correlation sensible heat flux to horizontal sensor separation in the unstable atmospheric surface layer, *J. Geophys. Res.*, *99*(D9), 18,545–18,553.

Lee, X., W. Massman, and B. E. Law (Eds.) (2004a), *Handbook of Micrometeorology: A Guide for Surface Flux Measurement and Analysis*, 250 pp., Kluwer, Dordrecht, Netherlands.

Lee, X., Q. Yu, X. Sun, J. Liu, Q. Min, Y. Liu, and X. Zhang (2004b), Micrometeorological fluxes under the influence of regional and local advection: A revisit, *Agric. For. Meteorol.*, *122*(1-2), 111–124.

Mauder, M., and T. Foken (2004), Documentation and Instruction Manual of the Eddy Covariance Software Package TK2, in *Abt. Mikrometeorologie*, p. 45, Univ. of Bayreuth, Bayreuth, Germany.

Meyers, T. P., M. E. Hall, S. E. Lindberg, and K. Kim (1996), Use of the modified Bowen-ratio technique to measure fluxes of trace gases, *Atmos. Environ.*, *30*(19), 3321–3329.

Moriwaki, R., and M. Kanda (2006), Local and global similarity in turbulent transfer of heat, water vapour, and CO_2 in the dynamic convective sublayer over a suburban area, *Boundary Layer Meteorol.*, *120*(1), 163–179.

Oncley, S. P., C. A. Friehe, J. C. Larue, J. A. Businger, E. C. Itsweire, and S. S. Chang (1996), Surface-layer fluxes, profiles, and turbulence measurements over uniform terrain under near-neutral conditions, *J. Atmos. Sci.*, *53*(7), 1029–1044.

Oncley, S. P., et al. (2007), The energy balance experiment EBEX-2000. part I: Overview and energy balance, *Boundary Layer Meteorol.*, *123*(1), 1–28.

Papaioannou, G., C. Jacovides, and P. Kerkides (1989), Atmospheric stability effects on eddy transfer coefficients and on Penman's evaporation estimates, *Water Resour. Manage.*, *3*, 315–322.

Paulson, C. A., E. Leavitt, and R. G. Fleagle (1972), Air-sea transfer of momentum, heat and water determined from profile measurements during BOMEX, *J. Phys. Oceanogr.*, *2*(4), 487–497.

Pielke, R. A., Sr. (2001), *Mesoscale Meteorological Modeling*, 2nd ed., 676 pp., Academic, San Diego, Calif.

Poulos, G. S., et al. (2002), CASES-99: A comprehensive investigation of the stable nocturnal boundary layer, *Bull. Am. Meteorol. Soc.*, *83*(4), 555.

Pruitt, W. O., D. L. Morgan, and F. J. Lourence (1973), Momentum and mass transfers in the surface boundary layer, *Q. J. R. Meteorol. Soc.*, *99*, 370–386.

Rannik, l., P. Keronen, P. Hari, and T. Vesala (2004), Estimation of forest-atmosphere CO_2 exchange by eddy covariance and profile techniques, *Agric. For. Meteorol.*, *126*(1-2), 141–155.

Schotanus, P., F. T. M. Nieuwstadt, and H. A. R. DeBruin (1983), Temperature measurement with a sonic anemometer and its application to heat and moisture fluctuations, *Boundary Layer Meteorol.*, *26*, 81–93.

Steeneveld, G. J., A. A. M. Holtslag, and H. A. R. DeBruin (2005), Fluxes and gradients in the convective surface layer and the possible role of boundary-layer depth and entrainment flux, *Boundary Layer Meteorol.*, *116*, 237–252.

Steeneveld, G. J., T. Mauritsen, E. I. F. de Bruijn, J. V. G. de Arellano, G. Svensson, and A. A. M. Holtslag (2008), Evaluation of limited-area models for the representation of the diurnal cycle and contrasting nights in CASES-99, *J. Appl. Meteorol. Clim.*, *47*(3), 869–887.

Sun, J., S. P. Burns, A. C. Delany, S. P. Oncley, T. W. Horst, and D. H. Lenschow (2003), Heat balance in the nocturnal boundary layer during CASES-99, *J. Appl. Meteorol.*, *42*, 1649–1666.

Swinbank, W. C., and A. J. Dyer (1967), An experimental study in micrometeorology, *Q. J. R. Meteorol. Soc.*.

van Dijk, A., W. Kohsiek, and H. A. R. DeBruin (2003), Oxygen sensitivity of krypton and Lyman-alpha hygrometers, *J. Atmos. Ocean Technol.*, *20*, 143–151.

Verma, S. B., N. J. Rosenberg, and B. L. Blad (1978), Turbulent exchange coefficients for sensible heat and water vapour under advective conditions, *J. Appl. Meteorol.*, *17*, 330–338.

Vickers, D., and L. Mahrt (1997), Quality control and flux sampling problems for tower and aircraft data, *J. Atmos. Ocean Technol.*, *14*(3), 512–526.

Warhaft, Z. (1976), Heat and moisture flux in the stratified boundary layer, *Q. J. R. Meteorol. Soc.*, *102*, 703–707.

Webb, E. K., G. I. Pearman, and R. Leuning (1980), Correction of flux measurements for density effects due to heat and water vapour transfer, *Q. J. R. Meteorol. Soc.*, *106*, 85–100.

Wilczak, J. M., S. P. Oncley, and S. A. Stage (2001), Sonic anemometer tilt correction algorithms, *Boundary Layer Meteorol.*, *99*, 127–150.

Wilson, D. K. (2001), An alternative function for the wind and temperature gradients in unstable surface layers, *Boundary Layer Meteorol.*, *99*(1), 151–158.

Yang, F. L., H. L. Pan, S. K. Krueger, S. Moorthi, and S. J. Lord (2006), Evaluation of the NCEP Global Forecast System at the ARM SGP site, *Mon. Weather Rev.*, *134*(12), 3668–3690.

Zilitinkevich, P., and P. Calanca (2000), An extended similarity theory for the stably stratified atmospheric surface layer, *Q. J. R. Meteorol. Soc.*, *126*, 1913–1923.

C.-H. Ho and S.-J. Park, School of Earth and Environmental Sciences, Seoul National University, San 56-1 Shilim-dong Kwanak-gu, Seoul 151-747, Korea. (hoch@cpl.snu.ac.kr)

L. Mahrt, College of Oceanic and Atmospheric Sciences, Oregon State University, 104 COAS Administration Building, Corvallis, OR 97331-5503, USA.

S.-U. Park, Center for Atmospheric and Environmental Modeling, Seoul National University Research Park (Main Center-Room 515), San 4-2 Bongcheon-dong Kwanak-gu, Seoul 151-818, Korea.